Journal of *Marine Science and Engineering*

MDPI

Article

A Multi-Method Approach to Identify the Natural Frequency of Ship Propulsion Shafting under the Running Condition

Pengfei Xing [1], Lixun Lu [1], Guobin Li [1,*], Xin Wang [2], Honglin Gao [1], Yuchao Song [1] and Hongpeng Zhang [1]

[1] Marine Engineering College, Dalian Maritime University, Dalian 116026, China
[2] Marine Design & Research Institute of China, Shanghai 200011, China
* Correspondence: liguobin@dlmu.edu.cn

Abstract: In order to identify the natural frequency of ship propulsion shafting under the running condition, a multi-method approach that combines Duffing Oscillator, harmonic wavelet packet transform, and probability density function is proposed. An experimental investigation on the natural frequency of running propulsion shafting is conducted on the ship propulsion shafting test bench, and the natural frequency response of running propulsion shafting under different alignment states is obtained from the measured bearing vibration signal. The results show that the natural frequency of propulsion shafting can be excited under the running condition, but its response is feeble. When the alignment state of the propulsion shafting gradually changes with the elevation of the front stern bearing, the identified natural frequency of the propulsion shafting shows an upward trend. In contrast, its amplitude shows a downward trend. Therefore, the proposed approach can identify the natural frequency of the ship propulsion shafting from the measured bearing vibration signal under the running condition.

Keywords: ship propulsion shafting; natural frequency; running condition; identification

Citation: Xing, P.; Lu, L.; Li, G.; Wang, X.; Gao, H.; Song, Y.; Zhang, H. A Multi-Method Approach to Identify the Natural Frequency of Ship Propulsion Shafting under the Running Condition. *J. Mar. Sci. Eng.* **2022**, *10*, 1432. https://doi.org/10.3390/jmse10101432

Academic Editor: Joško Parunov

Received: 25 July 2022
Accepted: 29 September 2022
Published: 4 October 2022

1. Introduction

Ship propulsion shafting is a vital part of the ship power system, so its condition monitoring and fault diagnosis are effective means to ensure the reliable operation of the ship power system and realize the safety of ship navigation. Modal parameter identification is a common technical means for monitoring and diagnosis structures [1]. Research has showed that when a fault such as a misalignment occurs in the shafting, its inherent properties such as stiffness or damping would be altered [2]. It may cause a change in the natural frequency of the shafting. Therefore, the natural frequency can be used to monitor the running condition of the ship propulsion shafting. However, since it is difficult to obtain the natural frequency of the propulsion shafting in a running condition, monitoring the condition of the ship propulsion shafting by using its natural frequency is still a challenge in application.

Fortunately, the Operational Modal Analysis (OMA) technique has been widely used to solve the above problem in recent years. Using the OMA technique, the modal parameters of structures, whose inputs are unknown and difficult or even unable to be measured, such as wind turbines, bridges, and other civil structures, can be obtained from the output response of the structures [3]. The propulsion shafting is one of the main excitation sources of ship vibration and noise. Therefore, condition monitoring and fault diagnosis of shaft systems by analyzing vibration signals are the primary tools at this stage. In 2022, Wen et al. propose a composite method that is based on the ensemble empirical mode decomposition (EEMD) and coupled with the autocorrelation method (AM), the fast Fourier transform (FFT), which is mixed and applied to identify the fault information of marine shafting during its operating by hull vibration [4]. In 2019, Lech Murawski et al. monitored torsional vibrations in propulsion shaft systems using instantaneous angular

velocity measurements [5]. Moreover, the bearing vibration signal, which can be acquired easily by sensors in real-time, is one of the important output responses of the propulsion shafting during navigation. Therefore, it is a practical method to obtain the natural frequency through the bearing vibration signals. Unfortunately, the natural frequency cannot be obtained from the bearing vibration signals by using the current OMA techniques, such as frequency domain decomposition [6], stochastic subspace identification [7], and Eigensystem Realization Algorithm [8]. Natural frequency is the standard information obtained from dynamic tests [9]. However, it is rarely possible to identify the signal at the natural frequency in the vibration analysis of ship shafting. Most researchers have analyzed the effects of transverse and torsional vibrations on ship shafting [5,10]. The occurrence of faults in the shaft system of a ship is often more evident at this time, and early fault monitoring is not possible. One possible reason is that the natural frequency component may be weak, even lower than the environmental noise due to the unknown and uncontrollable input excitation. Therefore, novel approaches are required to obtain the natural frequency of the running propulsion shafting from the bearing vibration signals in situ.

Usually, the signals corresponding to the natural frequency are weak. Thus, the Duffing Oscillator and the harmonic wavelet packet transform (HWPT) are suitable for extracting the natural frequency. Duffing Oscillator is one of the classic nonlinear systems, which is sensitive to periodic signals and immune to noise. Thus, it is widely used in weak signal detection [11–13]. For example, the Duffing Oscillator can be used to detect the weak fault characteristic frequency of a rotor in an aero-engine [14]. Additionally, the harmonic wavelet is widely used to extract the weak signal from noise due to its good band-pass filtering performance, and the frequency ranges can be chosen very flexibly for the time-frequency analysis [15]. For example, the weak characteristic frequencies of rolling bearings can be extracted by the HWPT [16]. Therefore, the combination of Duffing Oscillator and HWPT is proposed to detect and extract the weak periodic signal from the bearing vibration signal of propulsion shafting. Further, since both the harmonic responses and natural frequency responses are periodic signals, they are difficult to distinguish by their time domain waveform and spectrum. Since the statistical properties of a harmonic response and narrow-band stochastic response of a structural mode are different [17], the probability density function (PDF) is used to distinguish the natural frequency and the harmonic response from the extracted periodic signals. Therefore, based on the proposed method, the natural frequency response of the propulsion shafting is obtained from the bearing vibration signal under the running condition, which provides an opportunity to study the relationship between the natural frequency of the propulsion shafting and its running state.

In order to verify the validity of the proposed method, the experiments were conducted on the ship propulsion shafting test bench under different alignment states in this paper. The bearing vibration signals of the propulsion shafting were collected during the experiments. The natural frequency response of the running propulsion shafting was obtained from the measured signals using an approach combining the Duffing Oscillator, HWPT, and PDF. Then, the variation of natural frequency response was investigated under different alignment states.

2. Experiments

2.1. Experimental Equipment

The natural frequency of the running propulsion shafting was identified on the ship propulsion shafting test bench, as shown in Figure 1. In Figure 1a, a driving motor (modal number: D1TP180L-6) with a rotating speed ranging from 0 to 1000 rpm, rated power of 15 kW, and a rated voltage of 380 V is connected with the input end of the transmission shaft through coupling to drive the rotation of the transmission shaft. The transmission shaft with a length of 3.1 m and a diameter of 43 mm was supported by three journal bearings (i.e., the intermediate bearing, the front stern bearing, and the aft stern bearing).

In order to change the alignment of the propulsion shafting, each bearing was installed on a worm gear screw lifter as shown in Figure 1b, and the height variation of the bearing was 0.25 mm for every revolution of the worm gear. In addition, a counterweight plate with a mass of 22 kg was installed at the output end of the transmission shaft.

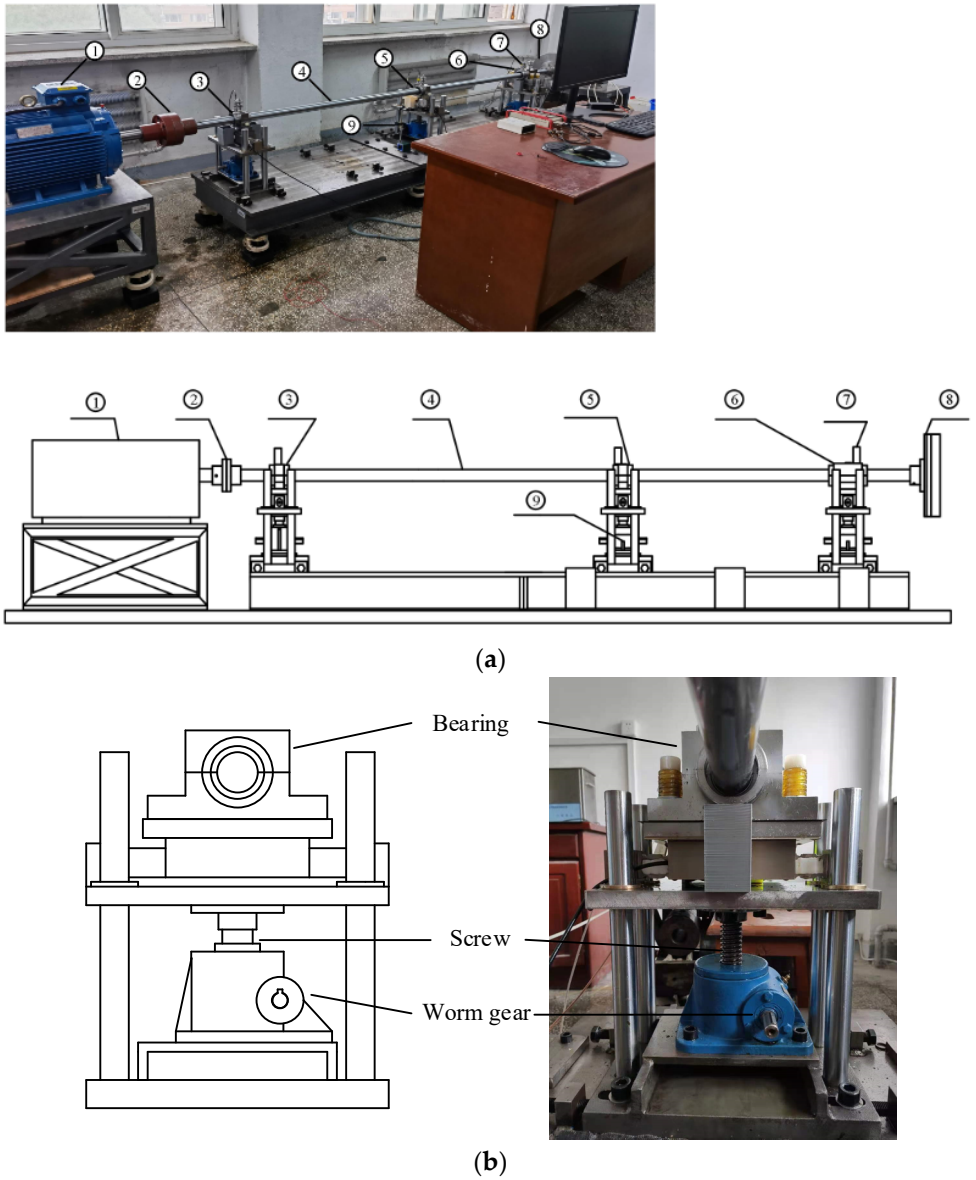

Figure 1. The ship propulsion shafting test bench. (**a**) Test bench: 1 Driving motor; 2 Coupling; 3 Intermediate bearing; 4 Transmission shafting; 5 Front stern bearing; 6 Aft stern bearing; 7 Acceleration sensor; 8 Counterweight plate; 9 worm gear screw lifter; (**b**) Worm gear screw lifter.

2.2. Experimental Set-Up

The stern front bearing changes had the most significant effect on the condition of the propulsion shafting test bench in this study. Therefore, different alignment states were obtained by changing the elevation of the front stern bearing, while leaving the other two bearings unchanged. Consequently, it was possible to analyze the vibration response of the shaft system in different states. During the experiments, the elevation of the front stern bearing was set to 0 mm under the linear alignment state, and then it was gradually increased from 0 mm to 1.2 mm with a step length of 0.2 mm. Thus, seven alignment states were obtained. What needs to be emphasized is that the rotating speed of the shaft was 90 rpm, and the running time at each alignment state was 10 min.

2.3. Collection of Vibration Signal

Three uniaxial acceleration sensors (model number: YA-22T) with a sensitivity of 506.2 mV/g, a range of 10 g, and a mass of 36 g were fixed on the bearing by means of magnetic adsorption to measure the vibration response. A data acquisition system (model number: NI Pxle-4499) was applied to collect the vibration signals from the uniaxial acceleration sensor with the sampling frequency of 2048 Hz and the sampling time of 10 s. Finally, we output the data to a personal computer (PC). During the experiments, a set of time series of vibration signals was collected every 20 s. At each alignment state, 20 groups of vibration signals were obtained. The schematic of this test experimental is depicted in Figure 2.

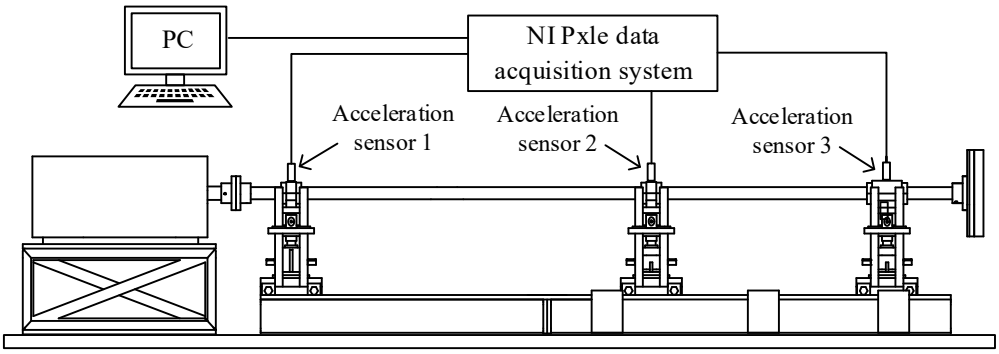

Figure 2. Schematic of Experimental Setup.

2.4. Measurement of Natural Frequency

Under the linear alignment state, the natural frequency of the non-running propulsion shafting was investigated by using the experimental modal analysis (EMA) method.

In this test, a single input single output (SISO)-type measurement was used, where the input excitation was applied to different excitation locations and a response was obtained at a fixed location to construct a single row of the frequency response function (FRF) matrix. The experimental setup consists of:

1. A uniaxial acceleration sensor (model number: YA-22T) was fixed on the output end of the transmission shaft to measure vibration response.
2. The sensitivity of and measurement range of the modal testing hammer (model number: YC-1160401) were 4 mV/N and 0–5 kN, respectively, and the material of the selected hammerhead was nylon.
3. Both the impact hammer and the acceleration sensor output were connected to the data acquisition (system model number: INV-3062T). The chassis was connected to the PC, and signals were acquired using DASP V10 (Figure 3).

The frequency range of interest in the experiment was 0–300 Hz. Due to the influence of frequency fluctuations on data collection, the analysis frequency was set to 500 Hz. Therefore, based on Shannon Sampling Theorem, and the sampling frequency of the acceleration sensor was set to 1280 Hz. In order to obtain a high-quality excitation pulse signal, the number of points within the pulse width of the force pulse was at least 20. Thus, the sampling frequency of the impact hammer sensor was set to 10,240 Hz. Figure 4 was a schematic of EMA experimental setup.

The shafting was marked with 33 excitation points, which were impacted by the hammer. It can be seen from Figure 4 that the vibration signal measurement point was designed near the counterweight plate. For these 33 excitation points, each excitation point was impacted three times, and the average value of these three signals was taken as the effective value. Each of the 33 data consisted of an output acceleration sensor response and an input impulse force imparted by the hammer. Thus, a unique frequency response function was obtained for each input and output combination: Figure 5a displays input and the output response of 33 measurements and the resulting FRF.

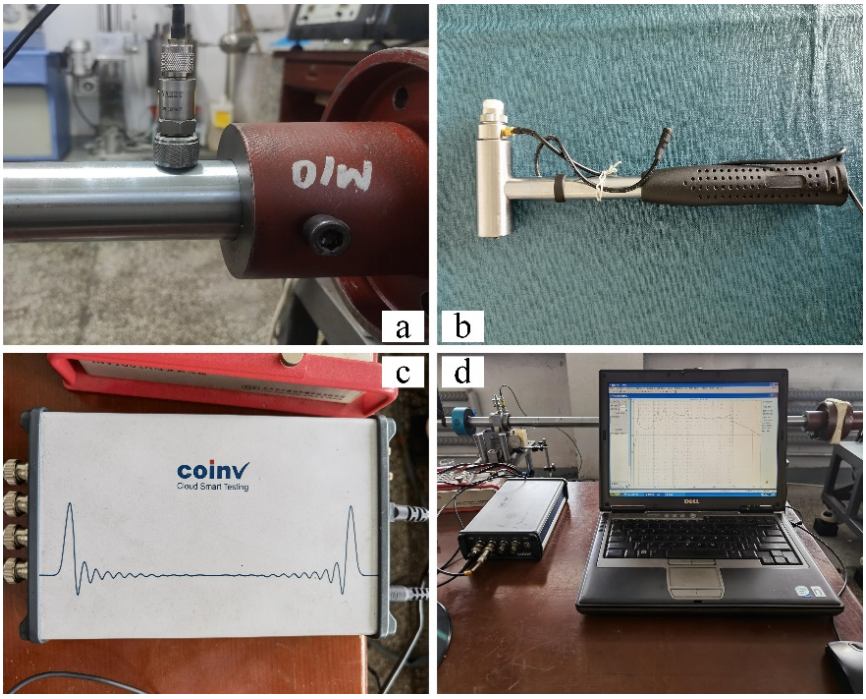

Figure 3. (**a**) Uniaxial acceleration sensor YA-22T; (**b**) Impact hammer YC-1160401; (**c**) Data acquisition system INV-3062T; (**d**) PC.

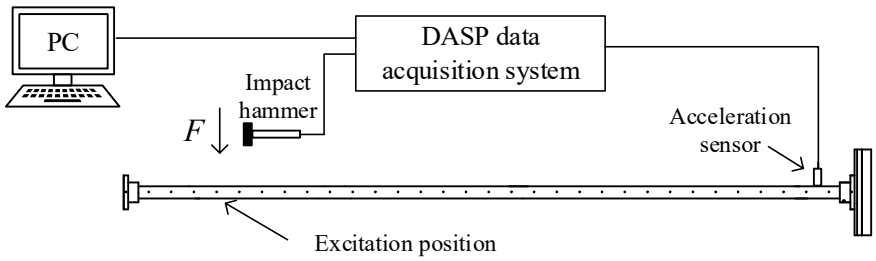

Figure 4. Schematic of EMA Experimental Setup.

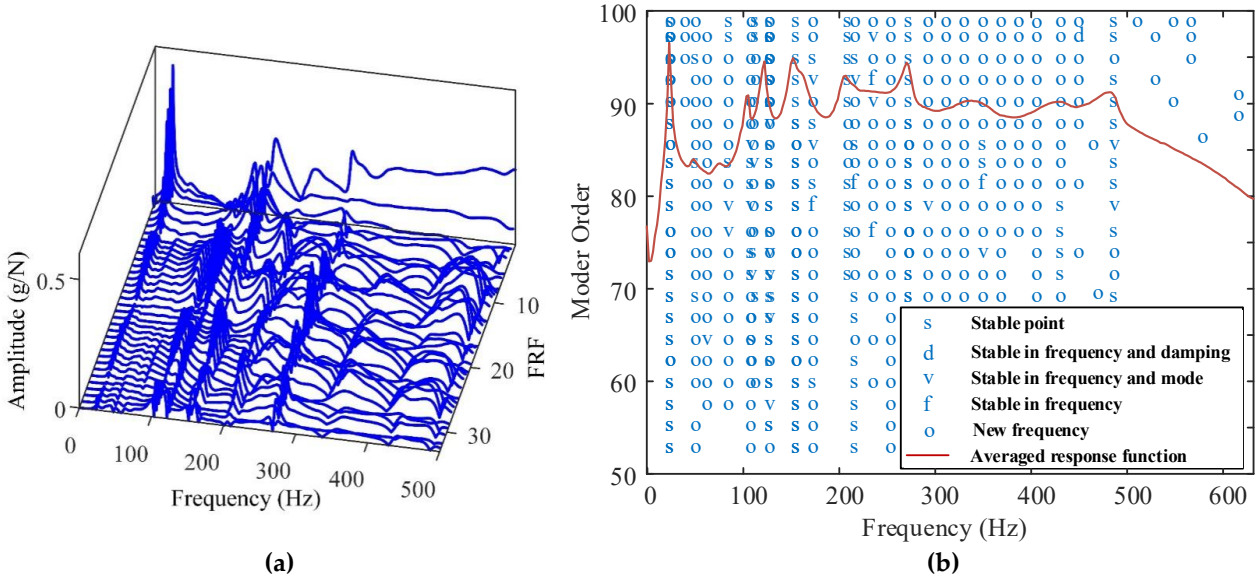

Figure 5. The eigensystem realization algorithm for modal parameter identification: (**a**) FRF of 33 excitation points; (**b**) Stabilization diagrams.

In this paper, Eigensystem Realization Algorithm was used to calculate the experimental modal of the propulsion shafting [8]. The Modal Assurance Criteria (MAC) and the stabilization diagrams (Figure 5b) were used as consistency indicators for modes and mode shapes [18]. The first six-order natural frequencies of the shafting were determined by the MAC value and the stabilization diagram, as shown in Table 1.

Table 1. Natural frequency of the non-running propulsion shafting under the linear alignment state.

Order-Number	1	2	3	4	5	6
Natural frequency/Hz	23.8	47.9	75.8	105.7	122.5	151.5

3. Implementation Approach

In this paper, Duffing Oscillator, HWPT, and PDF are used separately to detect, extract and identify the natural frequency of the running propulsion shafting from the measured vibration signals, and these methods are described below.

3.1. Detection

The Duffing equation can be expressed as follows:

$$\frac{\mathrm{d}^2x}{\mathrm{d}t^2} + c\frac{\mathrm{d}x}{\mathrm{d}t} - x + x^3 = \gamma\cos(t) \tag{1}$$

where c is the damping ratio, $\gamma\cos(t)$ is the reference signal, γ is the amplitude, ω is the angular frequency [11].

The ship propulsion shafting is a typical nonlinear dynamical system, and its dynamic natural frequency belongs to unknown frequency detection. Therefore, frequency transformation is performed in the Equation (1) to detect weak signals with different frequency components [19].

Defining $t = \omega_0\tau$, ω_0 is the reference frequency.

$$\begin{cases} \dot{x}(\tau) = \omega_0 y \\ \dot{y}(\tau) = \omega_0(-cy + x - x^3 + \gamma\cdot\cos(\omega_0\tau)) \end{cases} \tag{2}$$

By computation of the theoretical bifurcation value of Equation (1), we know that the chaotic motion is transforming into periodic motion when $R = \gamma_\mathrm{d}/c = 1.676889$. That is, if the amplitude of external exciting periodic force $\gamma = \gamma_\mathrm{d} = R{\cdot}c$ is or little less than this value, Equation (1) will experience chaotic and periodic motion alternately as time goes on [14]. Therefore, we derived from calculations in practice that the duffing oscillator isbest observed when the damping ratio is 0.5. The damping ratio can be in the range of 0~1. When the damping ratio c remains constant, there is a bifurcation value γ_d, and the Duffing Oscillator is in a critical state. When $\gamma < \gamma_\mathrm{d}$, the Duffing Oscillator remains in a chaotic state, as shown in Figure 6a; when $\gamma > \gamma_\mathrm{d}$, the Duffing Oscillator is in a large-scale periodic state as shown in Figure 6b.

The system produces mutation from chaos to a large-scale periodic state by utilizing periodic signal components to a system in a critical state, thereby realizing the detection of weak signals. Therefore, after setting the amplitude of the reference signal to γ_0, which is slightly smaller than the bifurcation value γ_d, the input signal is embedded into the Equation (2) to obtain:

$$\begin{cases} \dot{x}(\tau) = \omega_0 y \\ \dot{y}(\tau) = \omega_0(-cy + x - x^3 + \gamma_0\cdot\cos(\omega_0\tau) + input(\tau)) \end{cases} \tag{3}$$

The 'input' term represents the external forcing input to the oscillator. Weak periodic signals within the input signal are low amplitude signals in comparison to the reference signal [11,19,20].

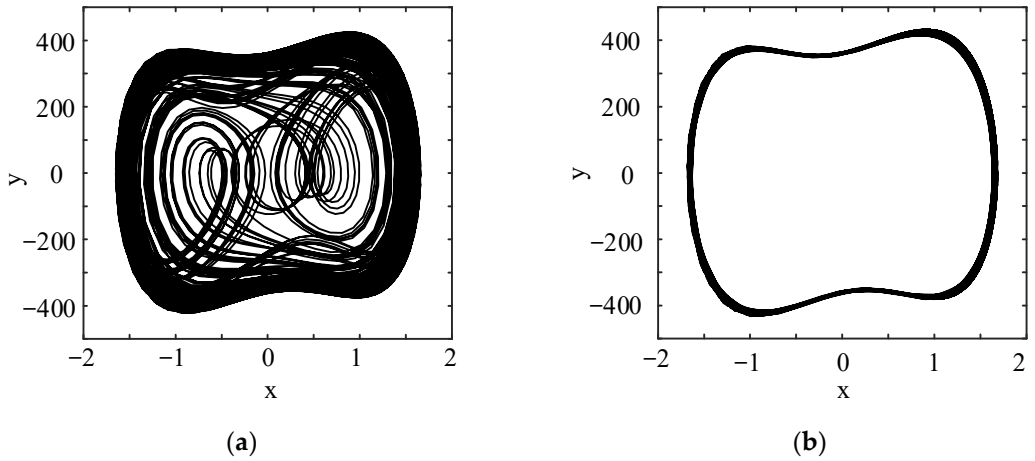

Figure 6. Phase trajectories of the Duffing Oscillator: (**a**) Chaotic state; (**b**) Periodic state.

The unknown frequency value of weak periodic signals embedded in the input signal is detected by frequency scanning based on the variable ω_0. If the frequency of the weak periodic signal is the same as the frequency of reference signal, the frequency of weak periodic signal could be detected by the Duffing Oscillator. The input signal can be defined as

$$input(\tau) = s(\tau) + N(\tau) \tag{4}$$

where, $s(\tau) = \gamma_1 \cdot \cos(\omega_1 \tau + \theta)$ is the weak periodic signal within the input signal, $N(\tau)$ is noise, γ_1 is the amplitude, ω_1 is the angular frequency, θ is the phase.

When the frequency of the weak periodic signal is the same as the reference signal frequency ($\omega_1 = \omega_0$), it can be detected by the Duffing Oscillator, and the total periodic signal of the Duffing Oscillator is:

$$\gamma' \cdot \cos(\omega_0 \tau + \varphi) = \gamma_0 \cdot \cos(\omega_0 \tau) + \gamma_1 \cdot \cos(\omega_0 \tau + \theta) \tag{5}$$

where, γ', φ respectively are the amplitude and the phase of the total signal.

If the total periodic amplitude is $\gamma' > \gamma_d$, the Duffing Oscillator only goes to the large-scale periodic phase. When the frequency of the external forcing input signal is different from the frequency of the reference signal, the Duffing Oscillator remains chaotic. Thus, the detection of weak periodic signals can be realized by applying the Duffing Oscillator.

3.2. Extraction

As an extension and translation of the harmonic wavelet transform (HWT), the HWPT has the excellent orthogonality and filtering characteristics of the HWT, and it can decompose a signal into an infinite number of signals with different refined frequencies. Although the energy is feeble, the signal in a frequency band of interest can be extracted by the HWPT. Therefore, the HWPT is used to extract the weak periodic signal detected by the Duffing Oscillator, and the process of HWPT is as follows.

Firstly, according to the frequency of the signal detected by the Duffing Oscillator, the number of layers j (j = 0, 1, 2, 3, . . . ,) of HWPT is determined, and then the bandwidth B in j layer can be written as:

$$B = 2^{-j} f_h \tag{6}$$

where f_h is the maximum analysis frequency of the signal. Let the upper and lower limits m and n of frequency band follow as:

$$\begin{cases} m = sB \\ \qquad\qquad s = 0, 1, 2 \ldots 2^j - 1 \\ n = (s+1)B \end{cases} \tag{7}$$

s is the index of the sub-band. Further, after determining the interested frequency band (m, n), the frequency-domain expression for the harmonic wavelet $\hat{\psi}_{m,n}$ is obtained:

$$\hat{\psi}_{m,n}[(n-m)\omega] = \begin{cases} 1/[(n-m)2\pi] & 2\pi m \leqslant \omega < 2\pi n \\ 0 & \text{other} \end{cases} \tag{8}$$

Then carry out Fourier transform on the measured signal $f(t)$ to obtain its discrete value in the frequency $\hat{f}(\omega)$. The frequency-domain expression of the discrete HWT is

$$\hat{W}(m, n, \omega) = \hat{f}(\omega)\hat{\overline{\psi}}_{m,n}[(n-m)\omega] \tag{9}$$

where $\hat{\overline{\psi}}_{m,n}[(n-m)\omega]$ is the conjugate of $\hat{\psi}_{m,n}[(n-m)\omega]$.

By taking the inverse Fourier transform of Equation (9), an equivalent expression of the HWT in the time domain can be expressed as

$$W(m, n, k) = (n-m)\int_{-\infty}^{\infty} f(t)\overline{\psi}_{m,n}\left(t - \frac{k}{n-m}\right)\mathrm{dt} \tag{10}$$

where k is the translation parameter, $k/(n-m)$ is the translation step of the harmonic wavelet, $\psi_{m,n}$ is the general expression of harmonic wavelet in the time domain, and $\overline{\psi}_{m,n}$ is the conjugate of the $\psi_{m,n}$.

Finally, the time domain signal W (m, n, k) in the interested frequency band (m, n) is got by the HWPT.

3.3. Identification

The ship propulsion shafting in operation usually presents harmonic excitation such as rotating frequency and its frequency multiplication. Therefore, the extracted periodic signal may be either the harmonic or natural frequency response. In order to obtain the natural frequency response of the ship propulsion shafting, the harmonic response needs to be identified and removed. In this paper, the PDF was used to distinguish between the natural frequency and harmonic response from the periodic signals extracted by the HWPT, and the method is described as follows.

The natural frequency response of the ship propulsion shafting can be considered as a linear superposition of responses under multiple random excitations [21], and its PDF $P_1(x)$ approximately obeys gauss distribution and can be expressed as

$$P_1(x) = \frac{1}{\sqrt{2\pi}\sigma}\mathrm{e}^{-\frac{(x-\mu)^2}{2\sigma^2}} \qquad (\mu > 0, \sigma > 0) \tag{11}$$

where μ is the mean of stochastic response variable x and σ is the standard deviation of x.

The harmonic response is a harmonic signal with periodic variations, and its PDF $P_2(x)$ is non-gaussian distribution and can be written as

$$P_2(x) = \frac{1}{\pi\sqrt{{x_0}^2 - x^2}} \tag{12}$$

According to Equations (11) and (12), the probability density curves of the stochastic and harmonic response were drawn, as shown in Figure 7. It can be observed from Figure 7 that the probability density curves were significantly different between the stochastic and harmonic responses. The stochastic response has only one peak, as shown in Figure 7a, while the probability density curve of the harmonic response contains two peaks, as shown in Figure 7b. Therefore, in this paper, the natural frequency response was determined by analyzing the shape of the probability density curve of the extracted periodic response signal, and then the harmonic response was eliminated.

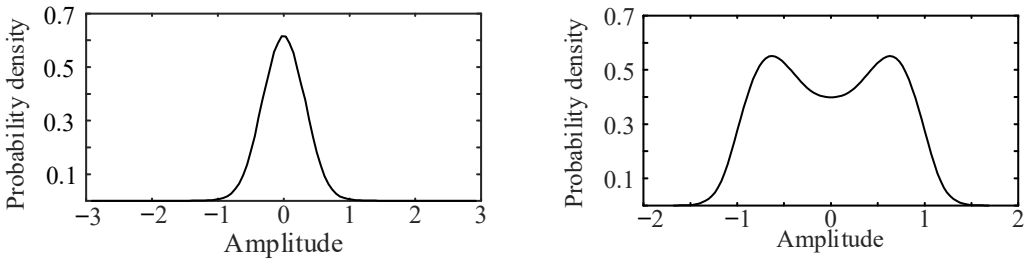

Figure 7. Probability density curve: (**a**) Stochastic response; (**b**) Harmonic response.

4. Results and Discussion

4.1. Acquisition of Natural Frequency Response

4.1.1. Analysis of Measured Signal

The bearing vibration signals are collected under the linear alignment state during the running of the propulsion shafting. Figure 8 is the time-domain waveform and spectrum of vibration signal measured from the intermediate, front, and aft stern bearing, respectively. It can be seen from Figure 8(Aa–Ca) that the measured vibration signal is an aliasing signal containing periodic and aperiodic components. Furthermore, it can be observed from Figure 8(Ab–Cb) that the natural frequency components such as 23.8 Hz are very weak, e.g., the first-order natural frequency of 23.8 Hz is almost submerged in the spectral line. Therefore, it is difficult to directly identify the natural frequency of the propulsion shafting from the bearing vibration signals.

4.1.2. Detection of Measured Signal

The natural frequency varies in a small range during the running of the propulsion shafting due to a limited effect of the running state on the natural characteristics of propulsion shafting. Based on existing research and related literature [2], the error between the natural frequency identified by the ship propulsion shafting under running conditions and the natural frequency obtained by the EMA is approximately 1.6%. In addition, bandwidth size has a significant impact on the efficiency of the calculation. This study considers the existence of errors and the efficiency of the calculation, and chose a bandwidth value of 3 Hz (1.98% of the sixth-order natural frequency of the EMA) after many numerical calculations. In practice, researchers can adjust the monitoring bandwidth according to the natural frequency of a real ship in its non-running state, reducing unnecessary frequency scanning. This, in turn, reduces the identification time and improves the real-time performance of the monitoring system. Therefore, the bandwidth of the detecting signal was chosen to be 3 Hz, and it is centered on the natural frequency measured by the EMA. According to the natural frequency of the non-running propulsion shafting measured by the EMA, the six frequency bands are determined, as shown in Table 2.

Table 2. The frequency bands for the detecting signal.

Order-Number	1	2	3	4	5	6
Natural frequency (Hz)	23.8	47.9	75.8	105.7	122.5	151.5
Detection band (Hz)	22.3~25.3	46.4~49.4	74.3~76.3	104.2~107.2	121.0~124.0	150.0~153.0
Reference signal amplitude	0.8265	0.8264	0.8263	0.8281	0.8305	0.8387

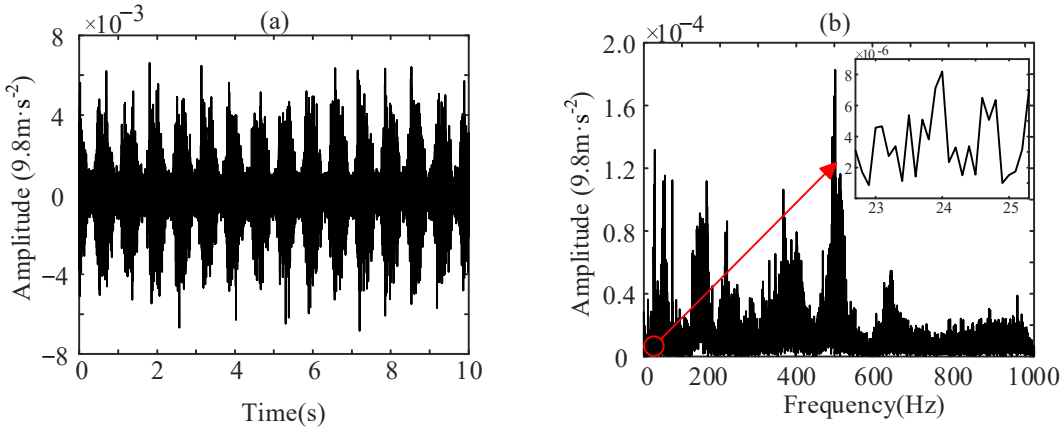

(A)

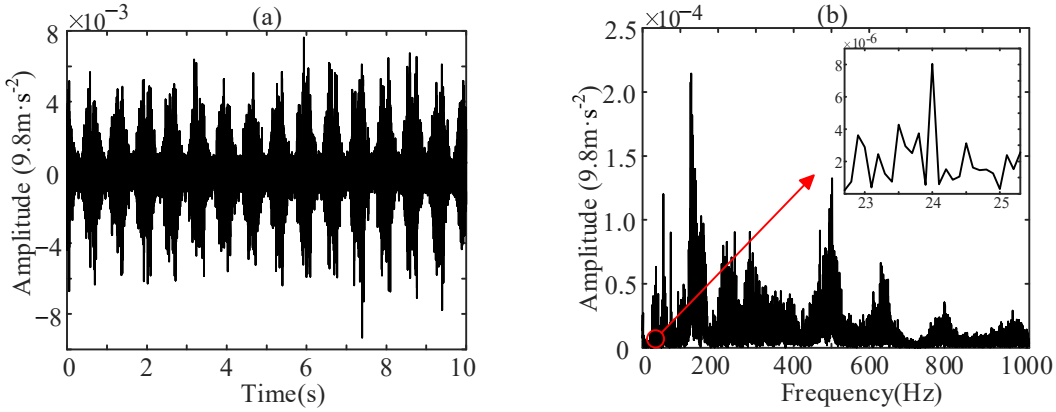

(B)

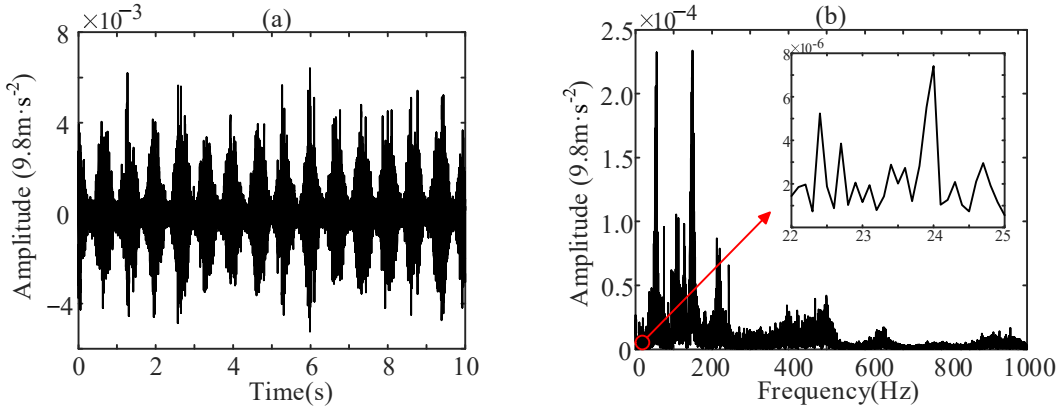

(C)

Figure 8. The time domain waveforms and frequency spectrum of the bearing vibration signal under the linear alignment state: (**A**) Intermediate bearing; (**B**) Front stern bearing; (**C**) Aft stern bearing.

To identify the weak periodic signals in different frequency bands, the six frequency bands generated are the range of variation of the reference frequency ω_0. The reference frequency ω_0 of the Duffing oscillator is varied in steps of 0.1 Hz within the six frequency bands to enable frequency monitoring of the bearing housing vibration signal. During the detection, the damping ratio c is chosen to be 0.5, and the amplitude of the reference signal in the different frequency bands is shown in Table 2. Under the linear alignment state, the vibration signal of the aft stern bearing in the frequency band of 22.3~25.3Hz is investigated, and the Duffing Oscillator's phase trajectories of the different detection

frequencies are shown in Figure 9. It is clearly observed from Figure 9 that the phase trajectory of 22.7 Hz, 22.9 Hz, 23.6 Hz, and 24.6 Hz are large-scale periodic states, and the phase trajectories of other frequencies remain chaotic. Therefore, four periodic signals with different frequencies in the frequency band of 22.3~25.3 Hz are detected by the Duffing Oscillator, and the periodic signals in other frequency bands are also detected, as shown in Table 3. It can be seen from Table 3 that the number of periodic signals detected in each frequency band is different.

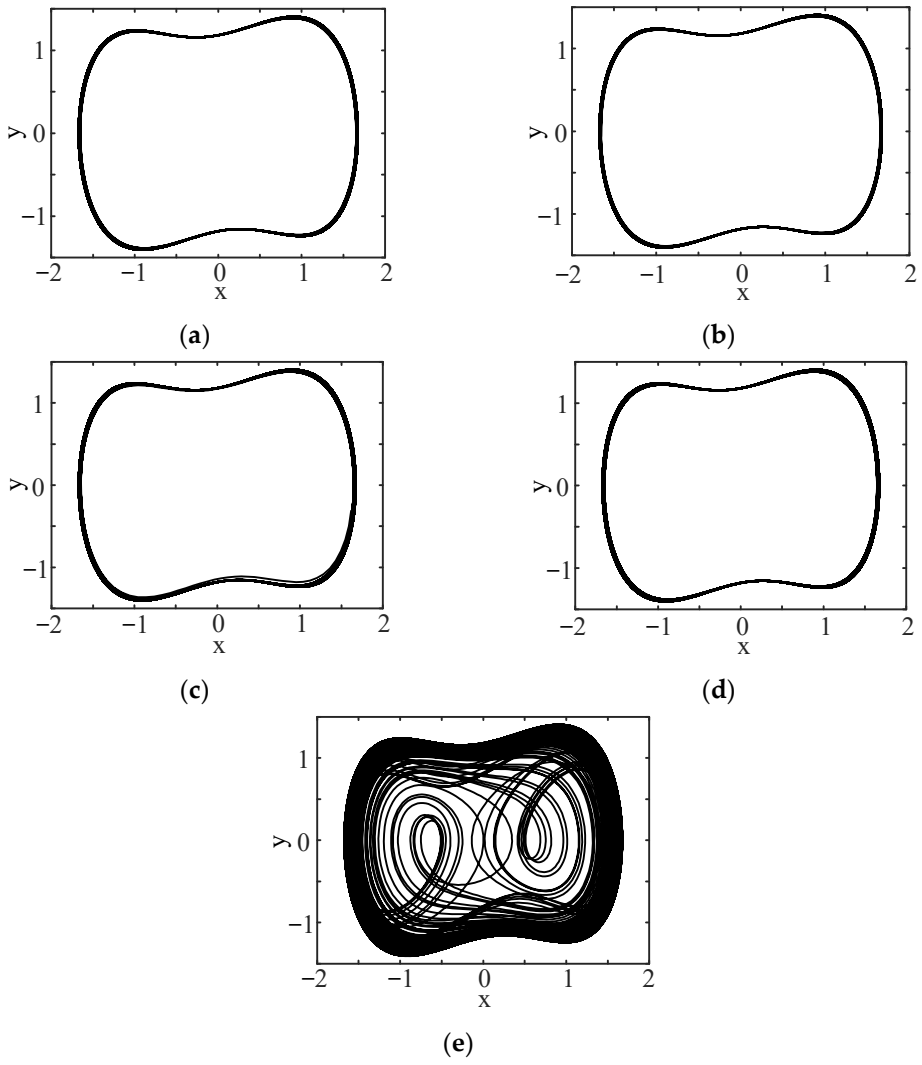

Figure 9. Phase trajectories of the Duffing Oscillator at 22.3~25.3 Hz: (**a**) 22.7 Hz; (**b**) 22.9 Hz; (**c**) 23.6 Hz; (**d**) 24.6 Hz; (**e**) Others.

Table 3. The frequency of the periodic signal detected in six frequency bands.

Frequency Band (Hz)	22.3~25.3	46.4~49.4	74.3~77.3	104.2~107.2	121.0~124.0	150.0~153.0
Frequency of the periodic signal (Hz)	22.7	47.0	75.4	105.1	121.8	150.4
	22.9	47.8	75.9	105.3	122.3	150.7
	23.6	48.1	76.2	105.5	122.5	151.3
	24.6	49.0				

4.1.3. Extraction of Weak Periodic Signal

To obtain the weak periodic signals with different frequencies, the HWPT is used to extract the weak periodic signals detected from the measured signals. Taking the

weak periodic signals detected with the frequency of 22.7 Hz, 22.9 Hz, 23.6 Hz, and 24.6 Hz as examples, a 13-layer HWPT is selected to decompose the measured signals into 8192 frequency sub-bands, and the bandwidth of each frequency sub-band is 0.125 Hz. The signals in the 181st (frequency band of 22.625~22.750 Hz), 183rd(frequency band of 22.875~23.000 Hz), 188th (frequency band of 23.500~23.625 Hz) and 196th (frequency band of 24.500~24.750 Hz) sub-bands are extracted as weak periodic signals respectively, as shown in Figure 10. It is clearly observed from the waveform in Figure 10A–D that all the extracted signals show periodic characteristics, and their spectrum is a line spectrum. Therefore, the weak periodic signals with different frequencies can be extracted using the HWPT. However, it is still difficult to distinguish between the harmonic signals the superimposed periodic signal.

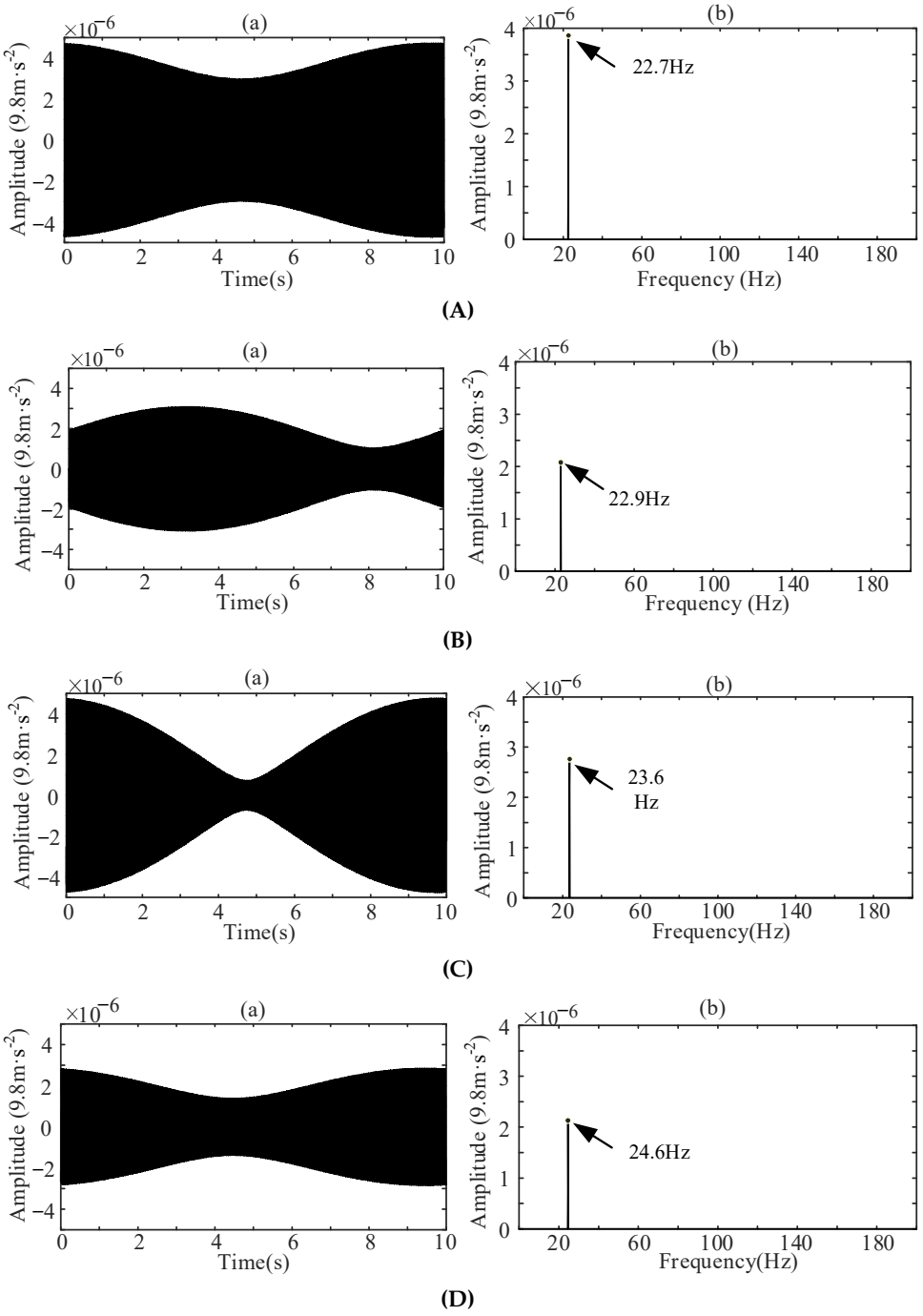

Figure 10. Time domain waveform and frequency spectrum of extracted frequency: (**A**) 22.7 Hz; (**B**) 22.9 Hz; (**C**) 23.6 Hz; (**D**) 24.6 Hz.

4.1.4. Identification of Extracted Signal

In order to distinguish the natural frequency and harmonic response from the extracted periodic signals, the amplitude probability distributions of the extracted periodic signals are calculated. Figure 11 shows the probability density curves of the extracted periodic signals with the frequency of 22.7 Hz, 22.9 Hz, 23.6 Hz, and 24.6 Hz. It is clearly observed that the probability density distribution of 23.6 Hz is a single peak curve as shown in Figure 11C and the others are double peak curves as shown in Figure 11A–C. According to the definition of PDF in Section 3.3 it can be suggested that the extracted periodic signal with the frequency of 23.6 Hz is a linear superposition response, i.e., 23.6 Hz is identified as the natural frequency. In this paper, based on the signals measured from the intermediate, front stern, and aft stern bearings, the first six-order natural frequencies of running propulsion shafting in the linear alignment state are obtained, as shown in Table 4. It can be seen from Table 4 that the obtained natural frequencies of the same order at different positions are close to each other, and their standard deviation is less than 1.

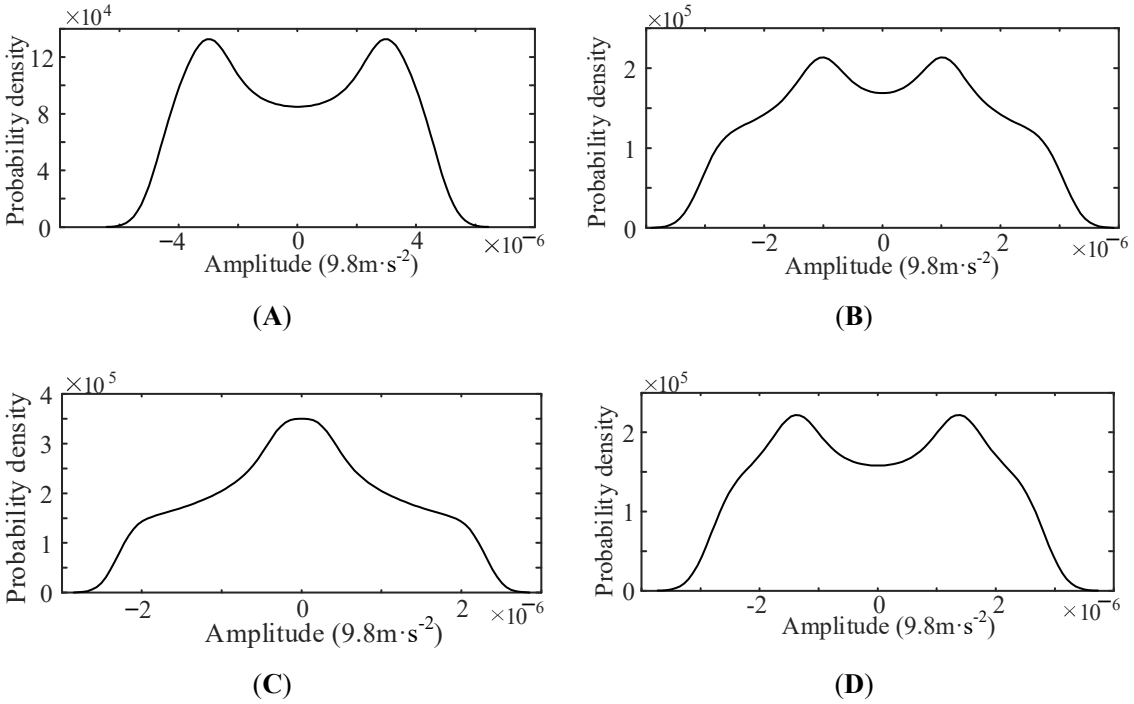

Figure 11. PDF of periodic frequency: (**A**) 22.7 Hz; (**B**) 22.9 Hz; (**C**) 23.6 Hz; (**D**) 24.6 Hz.

Table 4. Natural frequencies of running propulsion shafting in the linear alignment state.

Measuring Position \ Order-Number	1	2	3	4	5	6
Aft stern bearing/Hz	23.6	48.1	76.2	105.3	121.8	150.4
Front stern bearing/Hz	23.6	47.8	75.8	105.5	122.1	150.7
Intermediate bearing/Hz	23.1	47.5	75.0	105.3	122.2	150.4
Standard deviation	0.289	0.300	0.611	0.116	0.208	0.173

4.2. Variation of Natural Frequency Response under Different Alignment States

4.2.1. Frequency Changes

In order to investigate the variation of the natural frequency of the running propulsion shafting with alignment, the first six natural frequencies under different alignment states are obtained using the proposed approach combining the Duffing Oscillator, HWPT, and PDF. Figure 12 is the change of the natural frequency with the front stern bearing elevation. It can be clearly seen that the natural frequency of each order modal shows an upward trend with the increase of the front stern bearing elevation, as shown in Figure 12A−F

which implies that that the natural frequency is closely related to the axis position of the propulsion shafting and can be used to describe the alignment state.

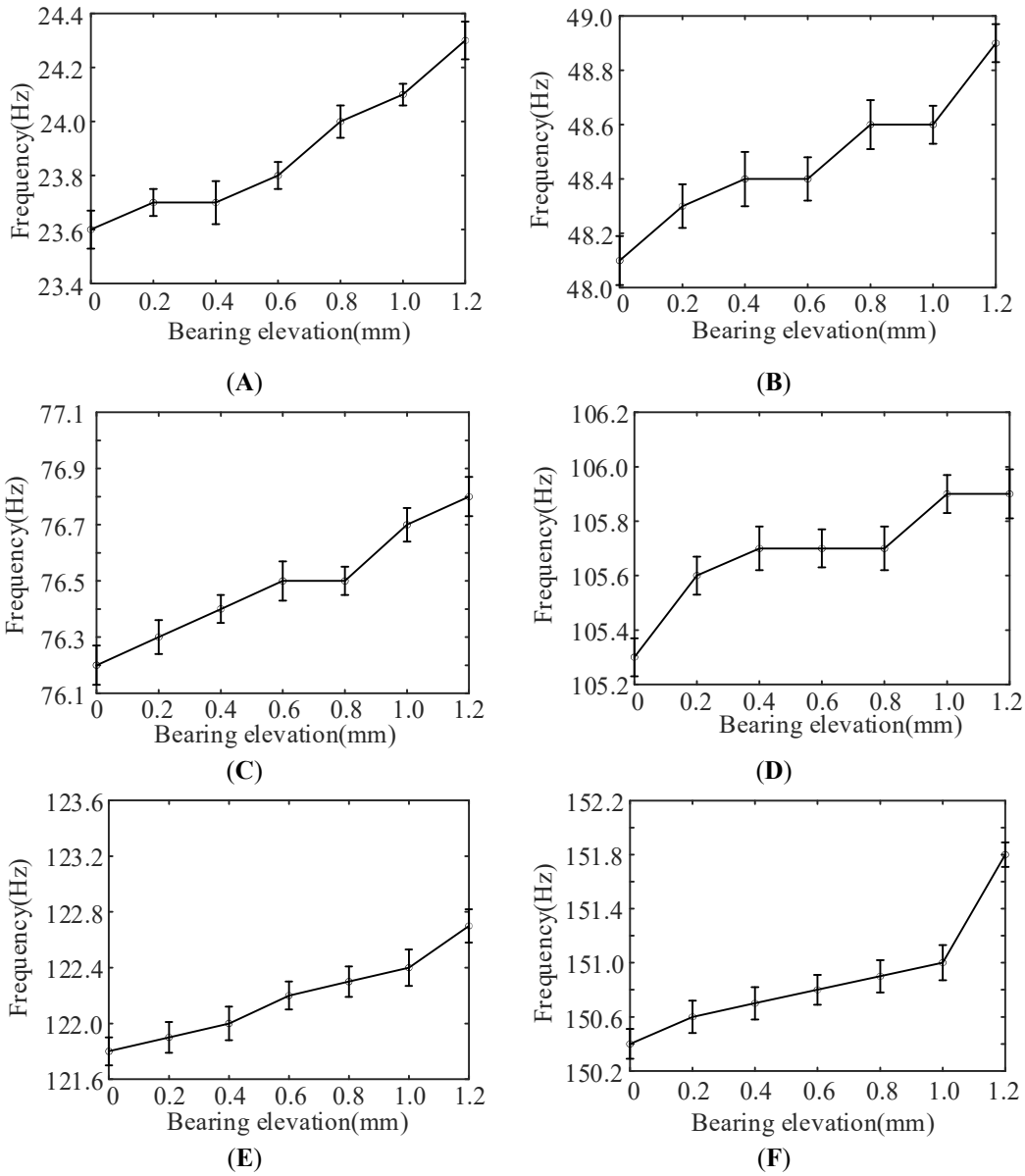

Figure 12. The change trend of the first six-order natural frequency: (**A**) First-order natural frequency; (**B**) Second-order natural frequency; (**C**) Third-order natural frequency; (**D**) Fourth-order natural frequency; (**E**) Fifth-order natural frequency; (**F**) Sixth-order natural frequency.

4.2.2. Amplitude Changes

Further, the natural frequency response signals are extracted, and the root mean square (RMS) values of their amplitudes are calculated, as shown in Figure 13. It can be observed that the amplitude RMS value of the natural frequency response signal at each order modal is very small and shows an obviously dropping trend with the increase of the front stern bearing elevation, as shown in Figure 13A−F. It indicates that the natural frequency response can be excited under the running of the propulsion shafting despite its weak intensity, and the natural frequency response signal can be used to characterize the alignment state.

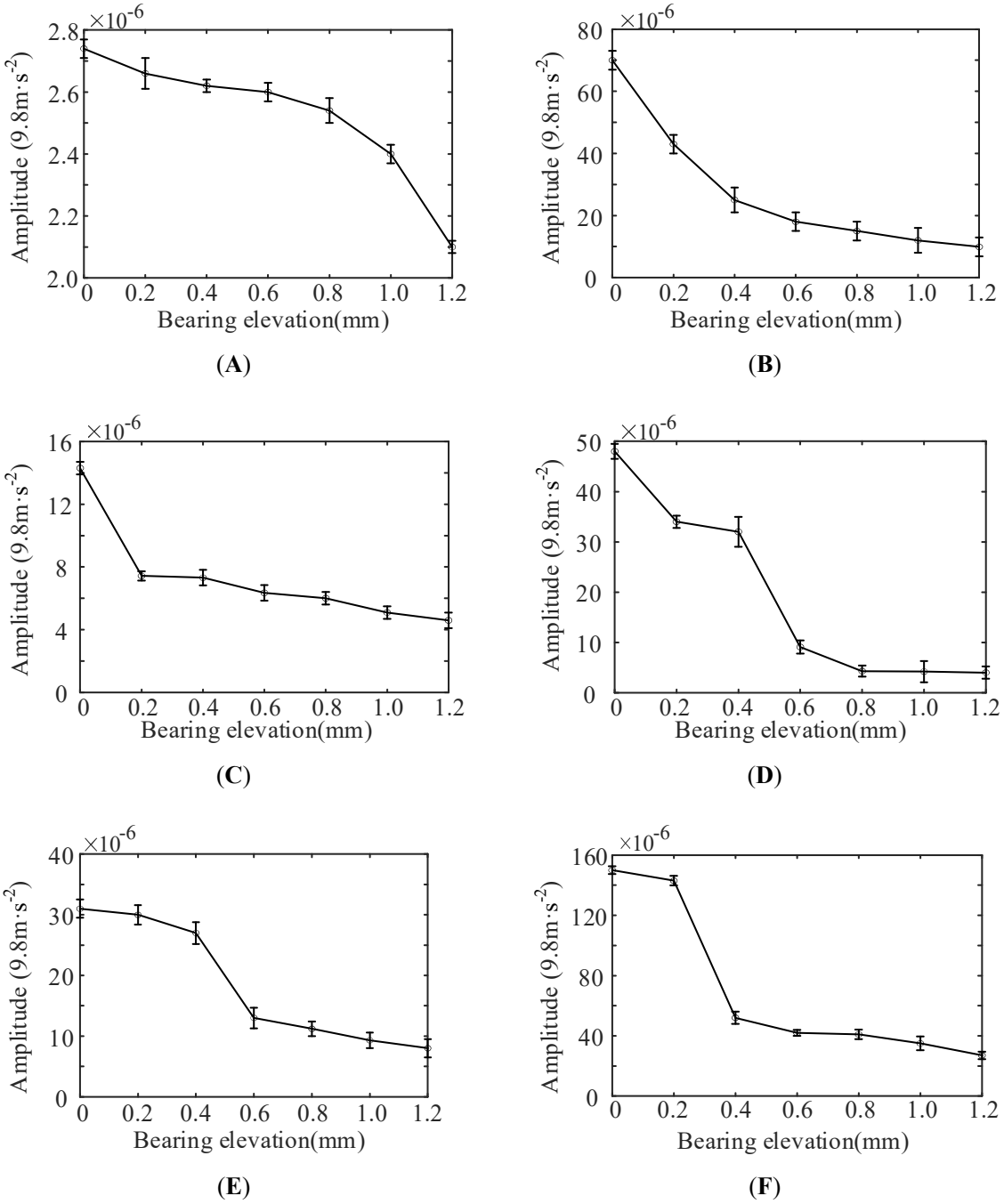

Figure 13. The amplitude change trend of the first six-order natural frequency: (**A**) First-order natural frequency; (**B**) Second-order natural frequency; (**C**) Third-order natural frequency; (**D**) Fourth-order natural frequency; (**E**) Fifth-order natural frequency; (**F**) Sixth-order natural frequency.

It is well known that when the axis position of the propulsion shafting changes, the stiffness of the propulsion shafting usually changes and the vibration form of the propulsion shafting also changes, such as the natural frequency of the propulsion shafting. This investigation shows that when the front stern bearing elevation gradually increases, the natural frequency of the propulsion shafting increases, and the amplitude decreases. Therefore, the natural frequency can be used to monitor the operating state of the propulsion shafting. It should be pointed out that the influence of the alignment on the propulsion shafting stiffness needs further investigation.

5. Conclusions

In this paper, a multi-method approach combining Duffing Oscillator, HWPT, and PDF was proposed to detect, extract and identify the natural frequency of the running propulsion shafting in a ship. By investigating the variation of natural frequency response under different alignment states, the following conclusions can be drawn:

1. Under the running condition, the natural frequency of the ship propulsion shafting can be excited, and the detection, extraction, and identification of the natural frequency can be achieved using a multi-method approach combining Duffing Oscillator, HWPT, and PDF.
2. When the propulsion shafting alignment changes gradually with the increase of elevation of the front stern bearing, the natural frequency increases, and the amplitude decreases. Therefore, the natural frequency can be used to monitor the operating state of the propulsion shafting.

In future studies, we will add various variables, such as motor speed, propeller mass, blade diameter, torque, bearing damage, and other failure modes. Further analysis of the variation in the natural frequency and its amplitude under these factors will enable condition monitoring of the natural frequency of the ship propulsion shafting, so that early fault characteristics can be detected in time. In addition, most vibration signal monitoring systems suffer from interference from ambient noise and other vibrating mechanical equipment. Therefore, noise reduction processing and rejection of interference mechanical equipment vibration frequency is part of the following research content. This method is somewhat inconvenient for cases in which the parameters of the monitoring equipment are unknown because of the need to identify the natural frequency of the monitored shaft system static in advance. However, with improvements in computer performance, the identification of static natural frequencies can be directly replaced by using a wide range of frequency scans. There is still a possibility of errors in this method because it requires manual screening of phase trajectory figures and probability density figures. Grayscale processing will achieve intelligent image recognition, eliminating manual screening's drawbacks.

Author Contributions: Conceptualization, P.X. and L.L.; methodology, X.W. and H.G.; validation, P.X., X.W., Y.S. and L.L.; formal analysis, G.L.; investigation, L.L.; resources, H.Z.; data curation, X.W. and H.G.; writing—original draft preparation, P.X.; writing—review and editing, L.L.; supervision G.L.; project administration, G.L.; funding acquisition, G.L. and P.X. All authors have read and agreed to the published version of the manuscript.

Funding: This research were funded by the National Natural Science Foundation of China, grant number 51879020, the Fundamental Research Funds for the Central Universities, grant number 3132022222.

Institutional Review Board Statement: Not applicable.

Informed Consent Statement: Not applicable.

Data Availability Statement: The data presented in this study are available on request from the corresponding author.

Conflicts of Interest: The authors declare that they have no known competing for financial interest or personal relationships that could have appeared to influence the work reported in this paper.

References

1. Zhang, Y.; Lian, J.; Liu, F. An improved filtering method based on EEMD and wavelet-threshold for modal parameter identification of hydraulic structure. *Mech. Syst. Signal Process.* **2016**, *68*, 316–329. [CrossRef]
2. Wang, Z.; Zhang, C.; Tian, Z. Ship Propulsion Shafting Status Monitoring Based on Operational Modal Analysis. *Ship Eng.* **2017**, *39*, 183–186+248. [CrossRef]
3. Xu, Y.F.; Zhu, W.D. Operational modal analysis of a rectangular plate using non-contact excitation and measurement. *J. Sound Vib.* **2013**, *332*, 4927–4939. [CrossRef]

4. Wen, X.; Meng, W.; Sun, X.; Zhou, R. A Composite Method of Marine Shafting's Fault Diagnosis by Ship Hull Vibrations Based on EEMD. *Shock Vib.* **2022**, *2022*, 1236971. [CrossRef]
5. Murawski, L.; Dereszewski, M. Theoretical and practical backgrounds of monitoring system of ship power transmission systems' torsional vibration. *J. Mar. Sci. Technol.* **2020**, *25*, 272–284. [CrossRef]
6. Brincker, R.; Zhang, L.; Andersen, P. Modal Identification from ambient Responses Using Frequency Domain Decomposition. 2000. Available online: https://vbn.aau.dk/ws/portalfiles/portal/12765845/Modal_Identification_from_Ambient_Responses_using_Frequency_Domain_Decomposition (accessed on 24 July 2022).
7. Van Overschee, P.; De Moor, B. Subspace algorithms for the stochastic identification problem. *Automatica* **1993**, *29*, 649–660. [CrossRef]
8. Juang, J.-N.; Pappa, R.S. An eigensystem realization algorithm for modal parameter identification and model reduction. *J. Guid. Control Dyn.* **1985**, *8*, 620–627. [CrossRef]
9. Mignolet, M.P.; Soize, C. Nonparametric stochastic modeling of linear systems with prescribed variance of several natural frequencies. *Probabilistic Eng. Mech.* **2008**, *23*, 267–278. [CrossRef]
10. Xue, S.; Wu, S.; Tang, Q.; Liu, S.; Liu, B. Research on torsional vibration monitoring system of ship power shafting. *IOP Conf. Ser. Mater. Sci. Eng.* **2021**, *1207*, 012007. [CrossRef]
11. Akilli, M. Detecting weak periodic signals in EEG time series. *Chin. J. Phys.* **2016**, *54*, 77–85. [CrossRef]
12. Akilli, M.; Yilmaz, N.; Akdeniz, K.G. Automated system for weak periodic signal detection based on Duffing oscillator. *IET Signal Process.* **2020**, *14*, 710–716. [CrossRef]
13. Wang, K.; Yan, X.; Yang, Q.; Hao, X.; Wang, J. Weak signal detection based on strongly coupled Duffing-Van der Pol oscillator and long short-term memory. *J. Phys. Soc. Jpn.* **2020**, *89*, 014003. [CrossRef]
14. Hu, N.Q.; Wen, X.S. The application of Duffing oscillator in characteristic signal detection of early fault. *J. Sound Vib.* **2003**, *268*, 917–931. [CrossRef]
15. Heo, Y.; Kim, K.-j. Definitions of non-stationary vibration power for time–frequency analysis and computational algorithms based upon harmonic wavelet transform. *J. Sound Vib.* **2015**, *336*, 275–292. [CrossRef]
16. Yan, R.; Gao, R.X. An efficient approach to machine health diagnosis based on harmonic wavelet packet transform. *Robot. Comput.-Integr. Manuf.* **2005**, *21*, 291–301. [CrossRef]
17. Brincker, R.; Andersen, P.; Møller, N. An indicator for Separation of Structural and Harmonic Modes in Output-Only Modal Testing, Universidad Politécnica de Madrid. 2000, pp. 265–272. Available online: https://vbn.aau.dk/en/publications/an-indicator-for-separation-of-structural-and-harmonic-modes-in-o (accessed on 24 July 2022).
18. Nadkarni, I.; Bhardwaj, R.; Ninan, S.; Chippa, S.P. Experimental modal parameter identification and validation of cantilever beam. *Mater. Today-Proc.* **2021**, *38*, 319–324. [CrossRef]
19. Wang, G.; Chen, D.; Lin, J.; Chen, X. The application of chaotic oscillators to weak signal detection. *IEEE Trans. Ind. Electron.* **1999**, *46*, 440–444. [CrossRef]
20. Akilli, M.; Yilmaz, N. Study of weak periodic signals in the EEG signals and their relationship with postsynaptic potentials. *IEEE Trans. Neural Syst. Rehabil. Eng.* **2018**, *26*, 1918–1925. [CrossRef] [PubMed]
21. Dong, X.; Lian, J.; Yang, M.; Wang, H. Operational modal identification of offshore wind turbine structure based on modified stochastic subspace identification method considering harmonic interference. *J. Renew. Sustain. Energy* **2014**, *6*, 033128. [CrossRef]